Visualizations of the flow patterns in a closed loop flat plate PHP with channel diameter above the critical one and tested under microgravity

Vincent Ayel[1*], Lucio Araneo[2], Pietro Marzorati[2], Cyril Romestant[1], Yves Bertin[1] and Marco Marengo[3]

[1]*Pprime Institut CNRS – ENSMA – Université de Poitiers, UPR 3346, Futuroscope-Chasseneuil, France*
[2]*Politecnico di Milano, Dipartimento di Energia, Milano, Italy*
[3]*University of Brighton, School of Computing, Engineering and Mathematics, Brighton, UK*

Abstract

In this paper the experimental study on a flat plate pulsating heat pipe (FPPHP), tested under microgravity during the ESA 62nd parabolic flight campaign, is presented. The PHP is made of a thin copper plate, in which a unique multi-turned channel is machined, and then it is closed on its top face by a transparent borosilicate plate thanks to a glue layer properly disposed around each channel segment to avoid cross-channel leakages. The equivalent hydraulic diameter of the square channel (2.5 x 2.5 mm²) is above the critical diameter of the working fluid. This induces a stratification of the liquid/vapor phases under normal gravity, whatever the orientation. During the parabolic flight campaign, the FPPHP is tested under vertical orientation. During normal gravity phases, the fluid stratifies with the liquid in the bottom zones, and vapor at the top zones. Thus the thermo-hydraulic transfer mode in this operation was either purely pool boiling inside completely filled channels (at the edges of the PHP plate), or annular flow pattern inside empty channels (in the center of the PHP plate). During microgravity phases, the fluid distributed naturally into a slug-plug flow pattern, with almost immediate trend to dry-out, followed by fast fluid overall motions leading to heat and mass transfers from evaporator towards the condenser zone, caused by some liquid small plugs moving towards the evaporator. These periods of stop and start motion were consecutive during the 20s of microgravity, and led to associated temperature oscillations.

Keywords: Pulsating Heat Pipes; Flow Pattern; Microgravity; Visualizations.

1. INTRODUCTION

In this paper an experimental study is reported of a Closed Loop Flat Plate Pulsating Heat Pipe (FPPHP, Fig. 1) tested under ground, hyper and microgravity conditions. As it is widely accepted that complex flow patterns, ranging from slug flow to annular flow, occur in the adjacent tubes of pulsating heat pipes (PHP), initiated by local pressure instabilities [1-3], many parameters have a direct influence on their operation [4,5]. Such flow patterns have obviously effects on the total heat flux transferred from the heated to the cooled ends of the PHP. One of the most important parameter is the channel internal diameter permitting liquid/vapor phase division into liquid slugs and vapor bubbles separated by menisci [5]. Many other parameters deserve mention, including: number of turns, PHP dimensions, filling ratio and physical properties of the working fluid, applied heat power, and, more particularly in the context of this study, the inclination with respect to gravity (for ground test conditions) or, generally, the change in the value of acceleration (for example, for tests on board of an aircraft during a parabolic flight campaign and/or under microgravity conditions for space application).

One of the major issues of PHPs operating under microgravity conditions is the existence of slug flow pattern in the tube/channels, which cannot be evaluated according to the critical Bond number widely used in the literature in terrestrial conditions ($Bo_{crit} = [g(\rho_l - \rho_v)D_{crit}^2/\sigma]^{1/2} \leq 2$). This point will be discussed in the next section for the present FPPHP. However, if it has been demonstrated that capillary pulsating heat pipes can operate under microgravity conditions [6-9], a more recent study [10] showed that the flow pattern switched from stratified flow under normal or hyper gravity conditions to slug flow under microgravity conditions. This last research tested a 3 mm internal diameter tube PHP (above the critical diameter value fixed at around 1.66 mm for the tested fluid, FC72, at 20°C) with a transparent tube portion on the upper part of the bench above the condenser zone. Using the visualization, it was possible to capture that the bubbles were perfectly symmetrical, and such behavior promised encouraging results on PHP performances under microgravity: considering a slug flow pattern, the bigger the tube diameter, the lower the viscous and capillary pressures losses opposing the overall fluid motion, thus promoting the mass, momentum and heat transfers all along the tubes. However, one must keep in mind that the higher the tube diameter, the lower the capillary forces that also maintaining liquid plugs/vapor bubbles phase separation in a slug flow regime. The inertial forces linked to the fluid velocity will be in this case able to destabilize such configuration by breaking the

menisci, according to the Weber number criterion ($We = \rho_l v_l^2 D/\sigma$) or the criteria suggested by Garimella with the Reynolds number [10]. To summarize, when *operating pulsating heat pipes under microgravity conditions, a higher diameter should lead to better performances and higher power dissipation, but also to a premature dry-out due to lower capillary forces*. The present study is also devoted to try to clarify such issue, together with the design itself of the Flat Plate PHP. As already discussed in [9], considering a non-transparent copper FPPHP with channels hydraulic diameter of 1.65 mm, just below the critical one of 1.66 mm with FC72 at 20°C (see above), two major issues differentiate a FPPHP from a capillary tube PHP: on the one hand, square shape channels have sharp angles in the corners, acting like capillary grooves assisting the liquid flow back to the evaporator zone. On the other side they may provoke rupture of the cross-sectional menisci, resulting in a flow regime transition into an annular flow (for vertical orientation); on the other hand, transverse thermal spreading occurs between channels, due to the structure solid geometry continuity, leading to lower temperature gradients. This causes homogenization of the pressure differences in the channels, which are the main drivers of oscillations under slug flow pattern. FPPHPs tested under horizontal inclination and microgravity conditions consequently show often premature dry-out [11], more importantly for bigger channel dimensions, as discussed above.

From all these considerations, a semi-transparent glass/copper FPPHP with channel hydraulic diameter above the critical one has been tested on ground and under hyper and microgravity conditions during the ESA 62th parabolic flight campaign.

2. EXPERIMENTAL APPARATUS

The tested FPHP was obtained by machining a copper plate (width: 124 mm, length: 204 mm, thickness: 2.5 mm) with a single rectangular shaped groove (width: 2.5 mm, depth: 2 mm). This single groove forms a series of 11 U-turns in the evaporator (see Fig. 1, left). The copper plate was covered by a 5 mm thick transparent borosilicate glass (width: 120 mm, length: 200 mm), glued on the upper part thanks to a silicon glue (NUSIL CV7 2289 1P) chosen for its elastic properties considering the differential expansion between copper and borosilicate. The glue was deposited to guarantee perfect sealing and the adjacent channels where also sealed-off relative to one another. The thickness of the glue (0.5 mm) was controlled

using shims during heating (cure phase), providing a depth of the channels (copper + glue) of 2.5 mm, giving them square shape.

As regards the cross-sectional dimensions of the channel (hydraulic diameter: $D_h \approx 2.5$ mm), the existence of slug flow pattern cannot be evaluated in microgravity conditions according to the critical Bond Number, the latter giving a critical diameter of 1.66 mm at 20°C for FC72. However, the previous visualizations of Mangini et al. [10] showed that the fluid (FC72) naturally distributes itself into slugs and plugs flow patterns in a 3 mm inner diameter cylindrical tube during microgravity phases. On ground conditions, the dimensions of the channel lead to stratification, whatever the orientation. Thus, most likely the hydraulic behavior between ground and microgravity conditions will be also in the present case highly different, with a fast transition between them.
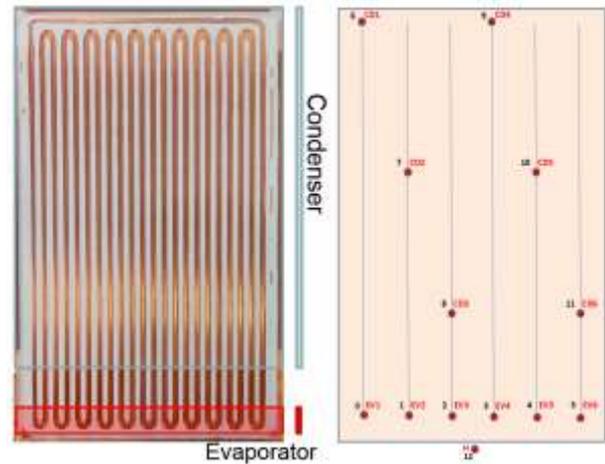

Fig. 1. Photograph of the front side of the FPPHP with heater and cold source positions (left), and sensor positions on its back side (right).

Sixteen T-type thermocouples of 0.5 mm (TC, ±0.5 K) monitor the temperature of each section in the PHP (Fig. 1, right): six thermocouples were glued in six grooves on the back side of the evaporator (T_{EV1}-T_{EV6}); six others were inserted in six grooves on the back side of the condenser (T_{CD1}-T_{CD6}); two thermocouples instrument the cooling fans inlet and outlet air temperatures; one measures the air temperature inside the heater containment (T_h) and the last one measures the aircraft ambient temperature (T_{air}). A pressure sensor (GE PTX5076-TA-A3-CA-HO-PS, 5 bars absolute, ±200 Pa) allows recording of local fluid pressure at the top of the condenser zone. A g-sensor (DE-ACCM3D, ±0.1g) is used to measure the gravity level variations during each parabolic

flight. Finally, a camera (XIMEA MG series Q3) is used, together with a mirror because of the confined low space, for the fluid flow pattern visualizations during PHP operation (Fig 2).
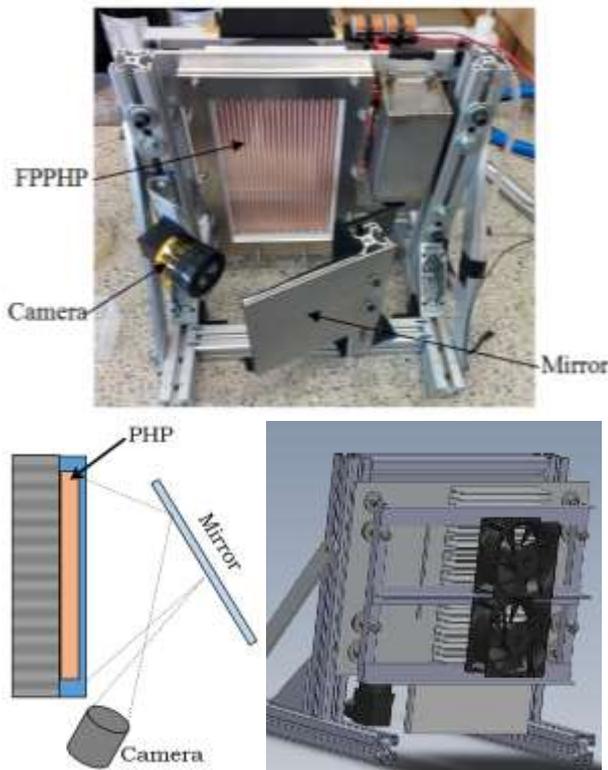

Fig. 2. FPPHP assembly: front side photograph (top); schematic views of PHP, mirror and camera (left/down) and back side with radiator fins and fans (right/down).

The evaporator zone of the FPPHP is heated by a wire electrical heater (Thermocoax Type ZEZAc10, 1 mm external diameter, $R = 3.8\ \Omega$) embedded in a serpentine groove machined in a copper plate of 10 x 120 mm² dimensions and 2 mm thick. The wire is connected to an electrical power supply (GWInstek® 3610 1, ±0.2 V). On the back side, the condenser section (160 x 120 mm²) is embedded in an aluminum heat sink cooled by means of two air microprocessor cooling fans (Fig. 2, down). Both heater and heat sink interfaces are wedged with thermal grease to reduce thermal contact resistance. Finally, the heater/heat sink and PHP elements are surrounded by PTFE plates and brackets to ensure double containment assembly for flight security purpose (Fig. 2).

Before being filled, the PHP was evacuated by means of an ultra-high vacuum system (ASM 142, Adixen by Pfeiffer Vaccum®). The working fluid was degassed in a tank by heating/cooling cycles until reaching the right value of filling mass

corresponding to the filling ratio at ambient temperature.

Finally, the operative conditions for all the ground and microgravity tests are:

- Working fluid: FC72, filling ratio: $FR \approx 50\%$;
- Heat power applied: from 20 W to 150 W;
- Cold source: air at plane ambient temperature ($T_{air} \approx 20°C$);
- Orientation: horizontal (ground tests only) and vertical bottom heated mode (BHM), according to the floor of the aircraft.

3. RESULTS AND DISCUSSIONS

3.1 Ground tests

Although the current device cannot be defined as a real pulsating heat pipe, given that its channel dimensions result in a phase stratification making impossible the standard slug flow pattern on ground, the authors thought interesting to present the results obtain for ground conditions (for vertical and horizontal orientations). Indeed, the unusual hydraulic behavior observed for both configurations deserves to be described in the two following paragraphs and helps make the difference with its operation under microgravity conditions.

3.1.1 PHP tested in vertical orientation

In this specific configuration, long time tests have been run for at least one hour, to reach nearly steady state conditions. The device is composed by different elements representing different thermal capacities connected in series by thermal resistances. The lighter elements like the copper plate and the fluid heat up quite rapidly, converging asymptotically to the temperature trends of the heavier and farthest elements like the heat sink. Some changes in the fluid distribution happening randomly from time to time modify the conductance properties and hence the temperatures of the components.

A typical long-time test is presented on Fig. 3 for the temperature and pressure measurements, with 100 W heat power applied. Note that only the most representative thermocouples have been plotted, in particular the two extreme temperatures for each zone (T_{EV1}, and T_{EV3}, for the colder, and hotter, temperatures of the evaporator zone, respectively, and T_{CD1}, and T_{CD3}, for the colder, and hotter, temperatures of the condenser zone, respectively). Note that the curves colors and associated sensors

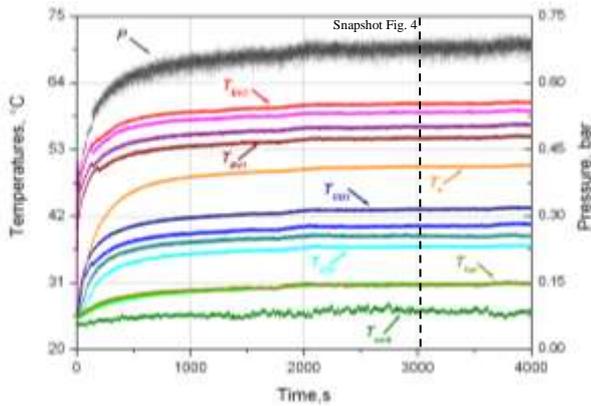remain the same than in Fig. 3 for all the following figures.

Fig. 3. Transient temperature/pressure responses of the FPPHP to a long time test at $Q = 100$ W (ground tests, vertical orientation).

Fig. 4 shows a snapshot of a movie corresponding to the test of Fig. 3, at time indicated by the vertical dashed line. Only the six right hand-side U-turns are represented. The authors apologize for the poor quality of the static picture. Only the movie may give a clearer and better representation of the phenomena occurring inside the FPPHP.
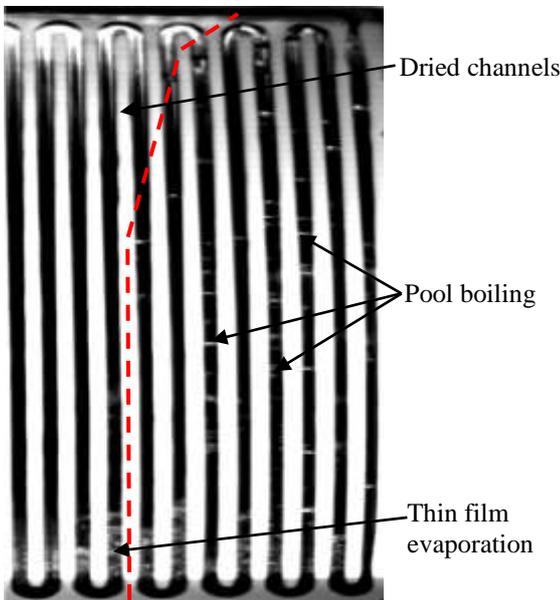

Fig. 4. Corresponding characteristic flow pattern in the right-half FPPHP at time indicated in Fig. 3 (ground tests, vertical orientation, $Q = 100$ W).

That said, when operated in vertical orientation, it appeared that each of the 11 couples of channels, together with their respective connecting lower U-turn, behave like boiling pools, interconnected each other by the top U-turns through which the vapor can move into the other channels. Because of the presence of a slight transversal temperature gradient, due either to a better cooling of the lateral channels that locally improves the vapor condensation or to edge effects that lead to higher temperature levels in the central zone of the evaporator, and because of the absence of any strong transversal redistribution and mixing phenomena, the liquid tends to migrate towards both sides of the FPPHP, leaving the central channels close to dry-out (separation indicated by the red dashed line on Fig. 4). Some vapor always condenses in the upper part of the central channels, with annular condensation that flows down towards the evaporator, as can be hinted by the thin film bursting on left-hand side of Fig. 4. On the contrary the colder lateral channels tend to get filled by liquid, and lead to pure pool boiling with bubbles rising all along the channels. The long path is composed by the two very lateral channels connected by the top horizontal that, due to its best cooling capability, tends to be completely flooded by liquid. Associated with its strong inertia, the latter helps to damp down the possible fluid oscillations through what should close the PHP closed loop.

3.1.1 PHP tested in horizontal orientation

In horizontal position the behavior is completely different. The liquid is no more vertically segregated, and the capillary forces are not able to maintain menisci that could contrast the gravity in such large channels; so the liquid spread naturally into a mixed gravity and capillary assisted channel flow. On the other side, the gravity pressure drop transverse to the channel is not strong enough to help the liquid flow back into the evaporator when subjected to heat power and vapor rising pressure. Consequently, the PHP tends to dry-out at much lower heat power inputs than in vertical orientation. Fig. 5 presents the temperature and pressure measurements for the FPPHP tested in horizontal orientation, with increasing heat power levels up to 120 W. Except for some oscillations noticed at the lower heat power level (here at 40 W, where some temperature fluctuations are noticeable on Fig. 5), the PHP operated dried, *i.e.* with all the liquid accumulated in the condenser region. This explains the smooth and flat curves observed for higher heat powers applied. The PHP then operates *practically* in pure conductive mode.
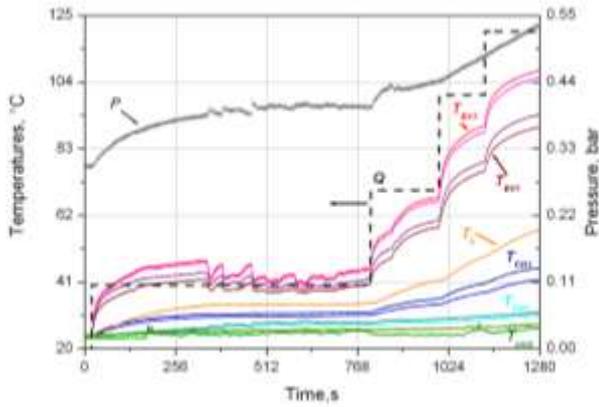
Fig. 5. Transient temperature response of the FPPHP to increasing levels of heat power (ground tests, horizontal orientation).

Fig. 6 shows an explanation of what was observed in the channels during horizontal operation. As mentioned above, as the evaporator zone tends to be dried-out, the liquid thus accumulates in the condenser region. However, in such "big" channels, gravity pressure drop ($\Delta P_g = \rho_l g D \approx 42$ Pa) assisted by capillary pressure drop ($\Delta P_c = \sigma/(D/2) \approx 9$ Pa) helps the liquid to flow back near to the evaporator zone as a flow channel-type. Such overall pressure drop is not sufficient enough to attain the evaporator, when the mass flow rate from the liquid "storage" is lower than the evaporation rate at the triple line downstream. One can also suggest here the existence of a Marangoni effect all along the liquid/vapor interface, the latter being subjected to an important temperature gradient from the condenser into the evaporator all along the channels.
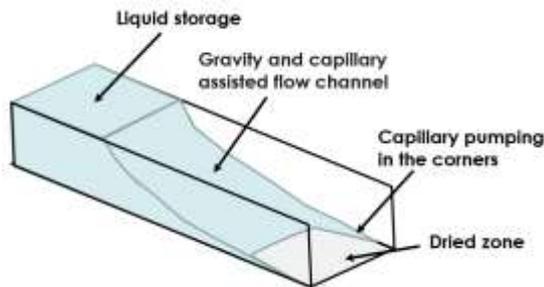

Fig. 6. Flow pattern in horizontal orientation.

Finally, note that a capillary pumping in the corners also helps the liquid to get closer to the evaporator. Due to all these factors, the presence of liquid close to the evaporator leads to thermal performance better than those of classical dried-out FPPHP with a sharp liquid/vapor frontier imposed by capillary forces, as observed in [11]. At low

heat powers, low frequency oscillations of temperatures and pressure observed in the PHP testify the slow dry-out and re-wetting phenomena. The vapor from the evaporator region moves above the stratified liquid and goes to condense, thus forming a slight pressure head that tends to slowly push back the liquid towards the evaporator. These oscillations fade away with increasing heat power.

3.2 Parabolic flight campaign

A parabolic flight campaign consists of three days of tests during which 31 parabolas trajectories are carried out every day, each of them giving a period of 22 s of microgravity (of around 0.1 ms^{-2}) preceded and followed by two periods of 20 seconds of hypergravity (at 1.8g, approximately).
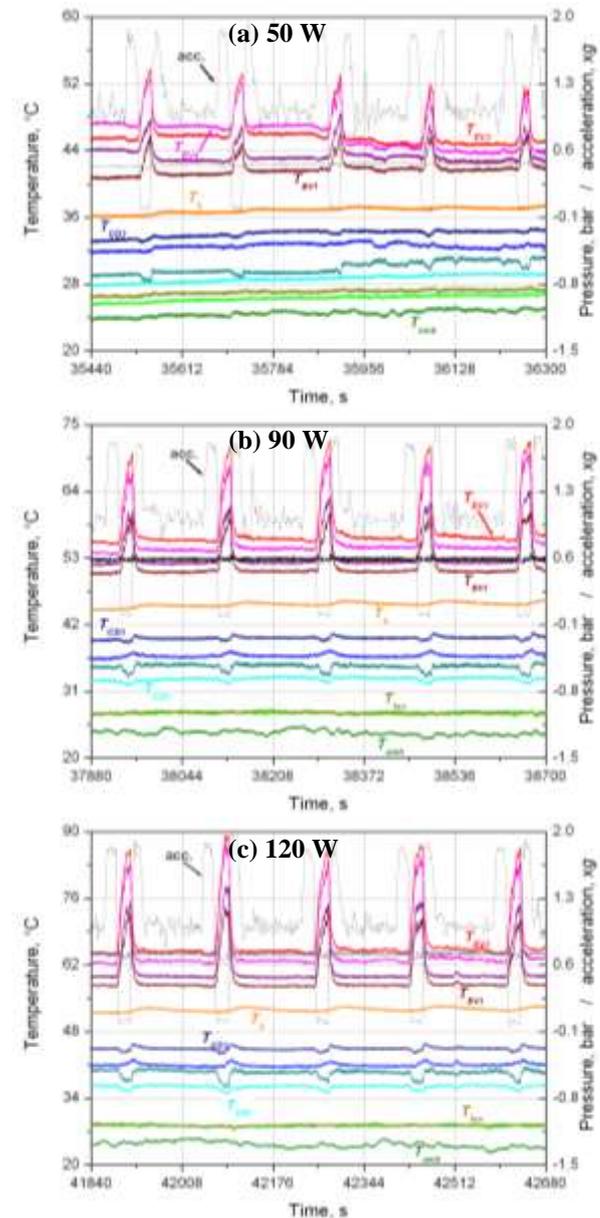
Fig. 7. Transient temperatures and pressure responses of the FPPHP to a series of 5 parabolas: (a) $Q = 50$ W; (b) $Q = 90$ W; (c) $Q = 120$ W.

During these tests, the FPPHP has been tested only in vertical orientation (BHM), varying the heat power applied every day, from 20 W to a maximum value of 150 W, with constant levels of heat power during each series of five consecutive parabolas. The following results are representative of the main thermal and hydraulic behavior observed during the parabolic flight campaign.

Foremost, in Fig. 7 are shown representative temperatures and pressure profiles for the FPPHP tested with three values of heat power (50, 90 and 120 W) applied each on a set of five successive parabolas. First observation is that temperatures rise in the evaporator zone together with their decrease in the condenser zone during microgravity phases. Furthermore, the evaporator temperature curves in microgravity are subject to some oscillations that will be explained below thanks to visualizations. A change in the flow pattern occurs and leads to performance degradation, compared to pool boiling/annular flow pattern in normal and hypergravity. Note that the hypergravity phases have practically no influence on the temperature fields and pressure signal, with slightly better performances as already observed in [9]. Increasing gravity improves heat transfers in such configuration: on one hand by increasing bubbles velocities relative to liquid one in pool boiling vertical channels; on the other hand by increasing the liquid film velocity, therefore its thickness, in middle dried channels subject to annular condensation, according to Nusselt condensation film theory.
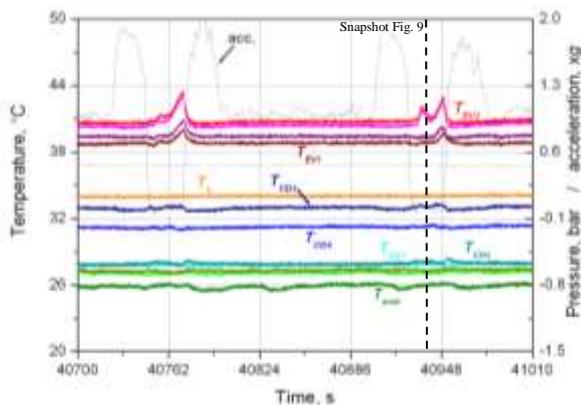
Except for the first curve at 50 W (Fig. 7a), the temperature response under normal or hypergravity present a feature of repeatability despite the change of fluid distribution resulting as a result of the microgravity phases. For the first case (Fig. 7a), one can notice a change in temperature profiles after the third parabola: the temperatures get closer the one to the others in the evaporator, and simultaneously slightly increase in the condenser. It has been observed that the flow pattern occurring in microgravity phase tends to homogenize the fluid distribution inside the whole PHP, before returning to segregated state in normal gravity for which the central channels are again partially filled with liquid.

Multiple bubbles train flow

Little bubbles arising from boiling inside liquid plugs crossing the evaporator
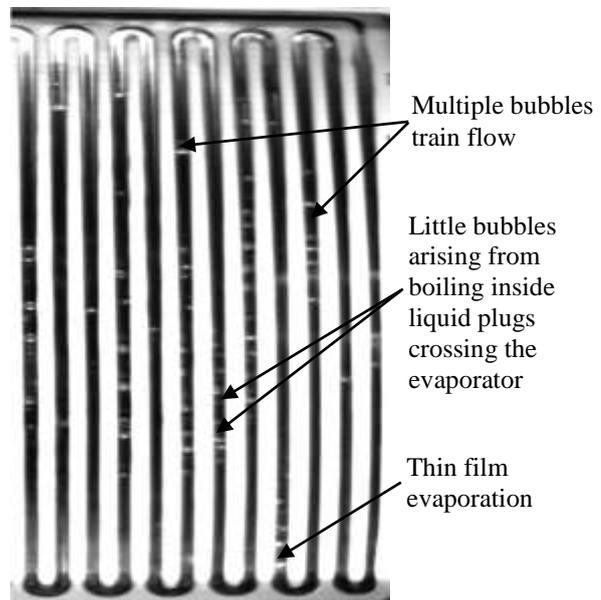
Thin film evaporation

Fig. 9. Corresponding flow pattern in the right-half FPPHP during microgravity conditions at time indicated by dashed line of Fig. 8 (parabolic flight, $Q = 30$ W).

To fully understand the phenomena occurring in microgravity, two cases will be presented, one at low heat power applied (30 W, Fig. 8 and 9), and the other at high heat power (150 W, Fig. 10 and 11). In the first case, Fig. 8 plots temperatures/pressure curves together with acceleration one as functions of time for two parabolas. One notes that the microgravity phases tend to increase the evaporator temperatures, but irregularly, and not all curves in the same time like in the second parabola of Fig. 8. So, there are periods of stops and starts operation that seem to be hardly reproducible. Fig. 9 presents a snapshot of a movie recorded during second parabola of Fig. 8, at time indicated by the vertical dashed line. Like in Fig. 4, only the six right hand-side U-turns are represented. The most important information

Fig. 8. Transient temperature responses of the FPPHP subject to two successive parabolas (parabolic flight, $Q = 30$ W).

here is that, *during microgravity, the flow pattern turns into slug flow, with consecutive liquid plugs and vapor bubbles invading the entire internal transverse section of the channels*, like Mangini et al. [10] with their 3 mm tube inner diameter PHP tested during parabolic flight campaign.

Despite the poor quality of the picture of Fig. 9, one can distinguish multiple bubbles trains in many channels. With no gravity forces, low capillary forces are sufficient enough to maintain liquid plugs between two vapor bubbles. Otherwise, due to very low capillary pressure drop (see section 3.1.1) and low viscous pressure losses (high hydraulic diameter) of the liquid plugs, these latters move very easily in the channels, so as to menisci that can break readily and destabilize the flow pattern. This results in two major behaviors in such configuration: first, *the fluid distribution tends spontaneously to a dry-out of the evaporator zone due to higher local pressures*; secondly, *isolated liquid plugs can easily move under the influence of small pressure instabilities around them*. By their motion some of them flow through the hot evaporator zone, leading to harsh evaporation increasing local pressure. This has the consequences of triggering the slug flow pattern motion in all FPPHP channels, thus temporarily improving the overall mass and heat transfers, diminishing the evaporator temperatures, until the following dry-out, and so on. Note also that some long liquid plugs crossing hot zones of the evaporator were subject to multiple consecutive bubbles boiling in the channel, as can be seen in Fig. 9.

before, the microgravity phase is accompanied by a harsh increase of the evaporator temperatures, during which fluctuations are clearly distinguishable. For all tested cases, an analysis of related videos showed that every fluctuations were associated to periods of stop-and-start, the "stops" corresponding to dries-out of the evaporator (increasing temperatures), the "starts" to triggering of the overall motion of the slug flow pattern in the FPPHP (decreasing temperatures). To illustrate this phenomenon, Fig. 11 presents a snapshot of a movie recorded during second parabola of Fig. 10, during a dry-out phase just before an overall massive motion. One can see down the left-end channel a 15 mm long liquid plug shifting to the evaporator (yellow arrow). Once reaching hot surfaces, a sudden evaporation appears and leads to a local pressure increase, which initiates the overall motion again, as mentioned before. However, dried-out and operating phases appear here with higher frequency than for lower heat powers applied.

Anyway, what can be remembered from these tests is that a slug flow pattern is possible under microgravity in cases where only segregated flow is possible on ground. The very low forces opposing liquid plugs motions lead to an almost immediate dry-out of the evaporator zone, but also to largely assisted movements of isolated small liquid plugs that resupply the evaporator in liquid evaporating thin films that restart the overall fluid motion in the FPPHP.
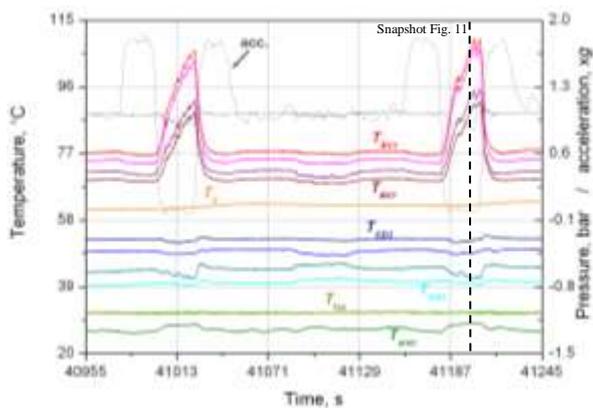

Fig. 10. Transient temperature responses of the FPPHP subject to two successive parabolas (parabolic flight, $Q = 150$ W).

Fig. 10 presents temperatures/pressure curves together with acceleration one as functions of time for a heat power applied of 150 W: as mentioned
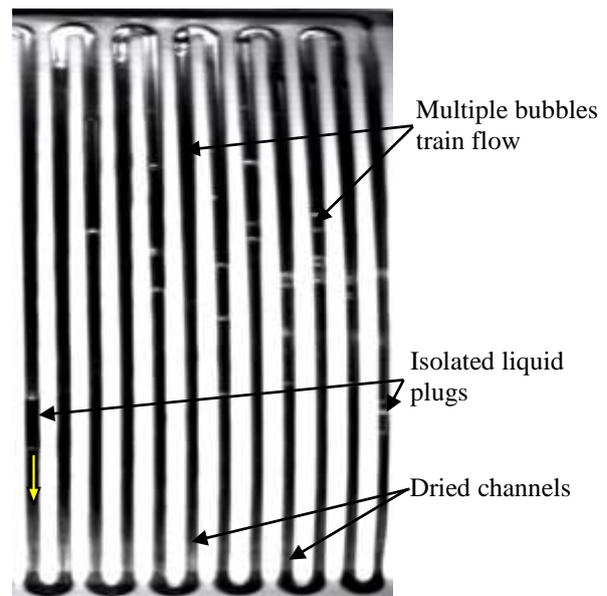

Fig. 11. Corresponding flow pattern in the right-half FPPHP during microgravity conditions at time indicated by dashed line of Fig. 10 (parabolic flight, $Q = 150$ W).

4. CONCLUSIONS

An experimental test on a ESA Parabolic Flight have been carried out for a Flat Plate Pulsating Heat Pipe. The FPPHP is made by a grooved copper plate covered by a glass layer, allowing visualization of the flow patterns for the different gravity and heat power conditions. The working fluid is a refrigerant (FC72) filling the channels at 50% FR. The present FPPHP has a hydraulic diameter higher than the so–called static capillary limit, linked to the Bond Number. Nevertheless in microgravity conditions, such capillary diameter ceases to have a physical meaning and the inertial forces become predominant. Since the new diameter threshold for slug-plug hydraulic regime can be higher than the static capillary limit, the FPPHP with a bigger diameter lead to better performances and higher power dissipation in microgravity conditions. On the other side high velocity oscillations are in this case more probable with the consequent break-up of the liquid menisci, i.e. the present FPPHP shows in a lower heat power limit for dry-out. The experimental test confirms that, even if on ground an evident fluid stratification is present, in microgravity the flow turns into slug-plug flow, with liquid slugs invading the entire internal transverse section of the channels. The gravity variation helps in maintaining the internal fluid oscillation and circulation. To notice, these tests have also enabled to highlight the role of local instabilities inducing mass and heat transfers inside the FPPHP, largely assisted by the very low pressure losses induced by liquid plugs moving inside channels with high hydraulic diameters, tests that would be impossible to observe under normal gravity.

NOMENCLATURE

Bo : Bond number
D : Diameter (m)
FR : Feeling ratio (%)
g : gravity acceleration (ms^{-2})
P : Pressure (Pa)
Q : Heat power (W)
T : Temperature (°C)
v : Velocity (ms^{-1})
We : Weber number

Greek symbols
ρ : Density (kgm^{-3})
σ : Surface tension (Nm^{-1})

Subscripts
air : ambient air
c/e : condenser/evaporator zones
crit : critical
h : hydraulic
l/v : liquid/vapor

REFERENCES

[1] Tong, B., Wong, T. and Ooi, K., Closed-loop pulsating heat pipe, *Applied Thermal Engineering*, 21 (2001) 1845-1862.

[2] Khandekar, S., Charoensawan, P., Groll, M. and Terdtoon, P., Closed loop pulsating heat pipes, part B: visualization and semi-empirical modeling, *Applied Thermal Engineering*, 23 (2003) 2021-2033.

[3] Liu, S., Li, J., Dong, X. and Chen, H., Experimental study of flow patterns and improved configurations for pulsating heat pipes, *Journal of Thermal Sciences*, 16 (2007) 56-62.

[4] Khandekar, S., Dollinger, N. and Groll, M., Understanding operational regimes of closed pulsating heat pipes: an experimental study, *Applied Thermal Engineering*, 23 (2003) 707-719.

[5] Charoensawan, P., Khandekar, S., Groll, M. and Terdtoon, P., Closed loop pulsating heat pipes, part A: parametric experimental investigations, *Applied Thermal Engineering*, 23 (2003) 2009-2020.

[6] Gu, J., Kawaji, M. and Futamata, R., Microgravity performances of icro pulsating heat pipe, *Microgravity Science and Technology*, 16 (2005) 181-185.

[7] Mameli, M., Araneo, L., Filippeschi, S., Marelli, L., Testa, R. and Marengo, M., Thermal response of a closed loop pulsating heat pipe under a varying gravity force, *International Journal of Thermal Sciences*, 80 (2014) 11-22.

[8] Iwata, N., Ogawa, H. and Miyazaki, Y., Visualization of Oscillating Heat Pipe under microgravity, *Proc. of 17th International Heat Pipe Conference*, Kanpur, India (2013) 6 p.

[9]   Ayel, V., Araneo, L., Scalambra, A., Mameli, M., Romestant, C., Piteau, A., Marengo, M., Filippeschi, S. and Bertin, Y., Experimental study of a closed loop flat plate pulsating heat pipe under a varying gravity force, *International Journal of Thermal Sciences*, 96 (2015) 23-34.

[10] Mangini, D., Mameli, M., Georgoulas, A., Araneo, L., Filippeschi, S. and Marengo, M., A pulsating heat pipe for space applications: Ground and microgravity experiments, *International Journal of Thermal Sciences*, 95 (2015) 53-63.

[11] Ayel, V., Romestant, C., Bertin, Y., Manno, V. and Filippeschi, S., Visualization of flow patterns in flat plate pulsating heat pipe: influence of hydraulic behaviour on thermal performances, *Proc. of 17th International Heat Pipe Conference*, Kanpur, India (2013) 6 p.